PHOTOCATALYTIC DECOLOURIZATION OF TEXTILE EFFLUENT BY USING METAL OXIDE NANOPARTICLES

NARAYANAPPA MADHUSUDHANA[1], KAMBALAGERE YOGENDRA[1], KITTAPPA M. MAHADEVAN[2]

Abstract. *In this study, textile effluent was selected for the photocatalytic decolourization studies under visible light irradiation. The two different nanoparticles, $CaZnO_2$-I was synthesized by solution combustion method using the fuel urea and $CaZnO_2$-II was synthesized by using acetamide. These nanoparticles were characterized by using X-ray diffraction (XRD) and Scanning Electron Micrograph (SEM). The average size was found to be 39 nm for $CaZnO_2$-I and 44 nm for $CaZnO_2$-II. The band gap of the nanoparticle $CaZnO_2$-I was found to be 2.57 eV and $CaZnO_2$-II was 2.67 eV. These nanoparticles were tested for the photocatalytic degradation of the selected textile effluent and the experiments were carried out by varying parameters such as catalyst concentration, pH and varying effluent concentration. At the same time, the efficiency of colour removal from the synthesized nanoparticles were compared with the procured TiO_2 of size < 25 nm.*

Keywords: *$CaZnO_2$, TiO_2, Photocatalyst, Nanoparticles, Violet GL2B, Decolourization.*

1. INTRODUCTION

Water is a precious natural resource that exists on planet earth, without which there would be no life. It is the basic requirement in all industrial processes. The wastewater has been generated by many industries *viz.,* textile, leather, pulp and paper, printing, photographs, cosmetics, pharmaceutical etc. Since, the textile industry used water as a primary medium for removing impurities, applying dyes and finishing agents, the main concern is therefore about the water discharged and the chemical load it carries. A number of chemicals that may be used in textile processes are worth mentioning for their potential negative effects on the environment and human health. These industries generate wastewater containing colour. Various types of dyes are used during manufacturing process, which contributes towards water pollution and leads to imbalance in bio-system [1-2].

In textile industry, dyes and their intermediates with high aromaticity and low biodegradability have emerged as major environmental pollutants [3-4] and nearly 10-15% of the dye is lost in the dyeing process and released into the effluent which is an important source of environmental contamination. Huge amount of water is used for dyeing and finishing of fabrics in the textile industries [5-6].

[1] Kuvempu University, Department of P.G studies and Research in Environmental Science, Jnana Sahyadri, Shankaraghatta, 577451 Shivamogga, India. E-mail: yogendraku@gmail.com.
[2] Kuvempu University, Kadur P.G Center, Department of Chemistry, 577451 Kadur, India.

Various physical, chemical and biological pre-treatment and post-treatment techniques have been developed over the last two decades to remove colour from dye contaminated wastewaters in order to cost effectively meet environmental regulatory requirements. Chemical and biological treatments have been conventionally followed till now. But these treatment methods have their own disadvantages. The heterogeneous photocatalytic degradation process is one of the most advantageous processes, because, it utilizes the UV/visible radiation in the photocatalytic processes to photo-excite the semiconductor catalyst in presence of oxygen. Under these circumstances oxidizing species, either bound hydroxyl radicals or free holes, are generated (Fig. 1). Using photocatalysis, organic pollutants can be completely mineralized reacting with the oxidizers to form CO_2, water of simple mineral acids. The process is heterogeneous because there are two active phases, solid and liquid. This process can also be carried out utilizing the near part of the solar spectrum ($\lambda < 380$nm) what transforms it into a good option to be used [7].
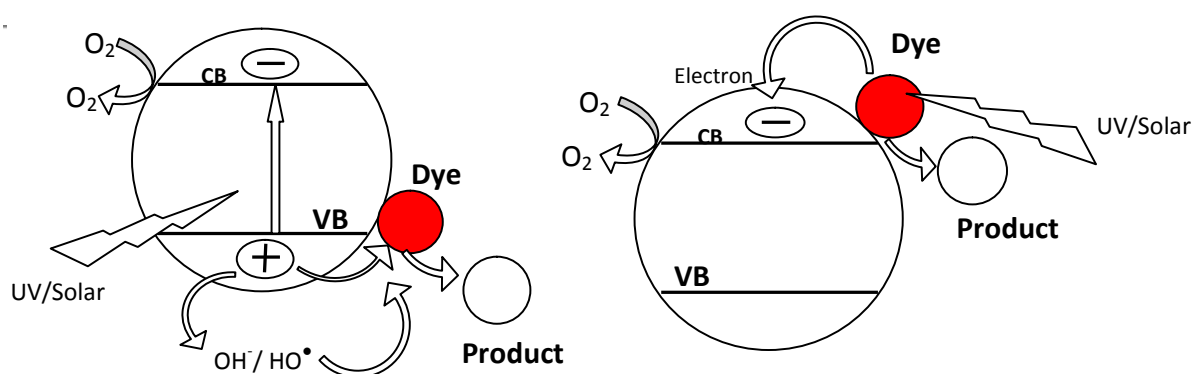
Fig. 1. Photo induced charge transfer processes in semiconductor nanoparticles.

Among the metal oxide photocatalysts, TiO_2 is most studied nanoparticles and frequently reported as an efficient photocatalyst in degrading many textile dyes. Many investigations have been carried out under UV radiation, since TiO_2 photocatalysts show relatively high activity and chemical stability under UV light [8] and absorbs only small portion of solar spectrum in UV region. On the other hand, ZnO has approximately same band gap energy (3.2 eV) as TiO_2 and its photocatalytic capacity has been anticipated to be similar to that of TiO_2. Further, some studies have confirmed that ZnO exhibits more efficiency than TiO_2. The biggest advantage of ZnO is that, it absorbs over a larger fraction of the solar spectrum than TiO_2 [9-12]. Similar studies have reported in our laboratory on different dyes [13-20].

So, in the continuation of our study TiO_2 of Size < 25 nm has been procured from sigma Aldrich and compared with the two different synthesized $CaZnO_2$ nanoparticles. The nanoparticle was characterized by X-ray diffraction (XRD) and Scanning Electron Micrograph (SEM) studies. The decolorization of one of the textile effluent solution (3%) was experimented in presence of sunlight irradiation.

2. MATERIALS AND METHODS

2.1. MATERIALS AND REAGENTS

The TiO_2 nanoparticle of size < 25 nm was procured from sigma Aldrich, Mumbai. $CaZnO_2$-I and $CaZnO_2$-II nanoparticles were synthesized in the laboratory by $Ca(NO_3)_2$ and $Zn(NO_3)_2$ using fuels urea and acetamide because they seem to be the convenient fuels which are easily available for the synthesis of the $CaZnO_2$ nanoparticles. The coloured textile effluent was collected form one of the textile industries. The chemicals like calcium nitrate $(Ca(NO_3)_2.4H_2O)$ (99%, AR), zinc nitrate $(Zn(NO_3)_2.6H_2O)$ (99%, A. R.), urea $(NH_2\ CO\ NH_2)$ (99%, AR) and acetamide (CH_3CONH_2) were obtained from Hi-media chemicals, Mumbai and used as received. The UV-VIS single beam spectrophotometer 119 (Systronics) has been used for recording absorbance at λ_{max}.

2.2. SYNTHESIS OF CALCIUM ZINCATE NANOPARTICLES BY SOLUTION COMBUSTION METHOD

The solution combustion process is an exothermic redox (oxidation and reduction reactions taking place simultaneously) reaction between an oxidizer and a fuel. When the heat is more evolved than the heat required for the reaction, the system becomes self-sustained. Also the exothermicity of such reactions takes the system to a high temperature. Hence, this process, popularly known as self-propagating high temperature synthesis is also called fire synthesis. The interesting feature of the process is that the sample once ignited continues to burn to consume itself [21].

The stoichiometry or the equivalence ratio $(\phi_e,\ O/F),$ at which the total combustion reaction takes place is very important and crucial. Combustion may not take place at all if the stoichiometry is not maintained. The calculation of the equivalence ratio is based on balancing the oxidizing (O) and reducing valency (F) of the reactants. The energy released by the combustion of the redox mixtures will be maximum when the equivalence ratio is $(\phi_e,\ O/F),$ unity (O is the total oxidizing and F the total reducing valency of the components). Here, the elements C, H and metal ions are considered as reducing species (*e.g.,* C = +4, H = +1, M^{2+} = +2, M^{3+} = +3, *etc.*). Oxygen is considered as oxidizer with a valency of –2. Nitrogen is considered to have zero valency [22].

2.2.1. Synthesis of $CaZnO_2$-I

The Calcium zincate nanoparticle was prepared by solution combustion method, using procured calcium nitrate, zinc nitrate, and Urea used as a fuel. Stoichiometric amounts of $Ca(NO_3)_2\ 4H_2O$ (7.08g) and $Zn(NO_3)_2\ 6H_2O$ (8.92g) were dissolved in a minimum quantity of water along with $(NH_2\ CO\ NH_2)$ (6g) in a silica crucible (with volume of 100 cm^3). The resulting mixture was introduced into the muffle furnace which was preheated to 600°C. The solution boils and undergoes dehydration followed by decomposition along with the release of certain amounts of gases it froths and swells forming foam which ruptures with a flame and glows to incandescence [23].

Table 1. Stoicheometric proportion used for the synthesis of CaZnO$_2$-I.

Mass of Ca(NO$_3$)$_2$ 4 H$_2$O	Mass of Zn(NO$_3$)$_2$ 6H$_2$O	Mass of NH$_2$CONH$_2$	Mass of Synthesized CaZnO$_2$-I
7.08g	8.92g	6 g	4.11g

The combustion reaction for the synthesis of CaZnO$_2$-I by the redox mixture method (urea) can be written as:

$$3Ca(NO_3)_2 + 3Zn(NO_3)_2 + 10NH_2CONH_2 \rightarrow 3CaZnO_2 + 10CO_2 + 20H_2O + 16N_2$$

The equivalance ratio (ϕ_e) in the above case is calculated as follows:

OV of $Ca(NO_3)_2$, $1Ca = +2$, $2N = 0$, $6O = -12$, Total $= +2 - 12 = -10$.

OV of $Zn(NO_3)_2$, $1Zn = +2$, $2N = 0$, $6O = -12$, Total $= +2 - 12 = -10$.

RV of NH_2CONH_2, $1C = +4$, $4H = +4$, $2N = 0$, $1O = -2$, Total $= +4 + 4 - 2 = +6$.

(ϕ_e, O/F) = 10/6 = 1.66 *i.e.,* for every one mole of Ca(NO$_3$)$_2$, 1.66 mole urea required.

(ϕ_e, O/F) = 10/6 = 1.66 *i.e.,* for every one mole of Zn(NO$_3$)$_2$, 1.66 mole urea is required.

For the synthesis of CaZnO$_2$-I the total number of moles of urea required is: 1.66+1.66= 3.32 mole (Fig. 2).

Fig. 2. Synthesized CaZnO$_2$-I at 600 °C.

2.2.2. Synthesis of CaZnO$_2$-II

The Calcium zincate nanoparticle was prepared by solution combustion method, using procured calcium nitrate, zinc nitrate, and Urea (Fuel). Stoichiometric amounts of metal nitrates, Ca(NO$_3$)$_2$.4H$_2$O (8.65g) and Zn(NO$_3$)$_2$.6H$_2$O (10.90g) along with the fuel (CH$_3$CO NH$_2$) (3.93g) in a silica crucible (with volume of 100 cm^3). The resulting mixture was introduced into the muffle furnace which was preheated to 600°C. The solution boils and undergoes dehydration followed by decomposition along with the release of certain amounts of gases it froths and swells forming foam which ruptures with a flame and glows to incandescence [24].

Table 2. Stoicheometric proportion used for the synthesis of CaZnO$_2$-II.

Mass of Ca(NO$_3$)$_2$ 4 H$_2$O	Mass of Zn(NO$_3$)$_2$ 6H$_2$O	Mass of CH$_3$CO NH$_2$	Mass of Synthesized CaZnO$_2$-II
8.65g	10.90g	3.93g	5.03g

The combustion reaction for the synthesis of CaZnO$_2$-II by the redox mixture method (acetamide) can be written as:

$$11Ca(NO_3)_2 + 11Zn(NO_3)_2 + 20CH_3CONH_2 \rightarrow 11CaZnO_2 + 40CO_2 + 50H_2O + 32N_2$$

The equivalance ratio (ϕ_e) in the above case is calculated as follows:

OV of $Ca(NO_3)_2$, $1Ca = +2$, $2N = 0$, $6O = -12$, Total $= +2 - 12 = -10$.

OV of $Zn(NO_3)_2$, $1Zn = +2$, $2N = 0$, $6O = -12$, Total $= +2 - 12 = -10$.

RV of CH_2CONH_2, $2C = +8$, $5H = +5$, $2N = 0$, $1O = -2$, Total $= +8 + 5 - 2 = +11$.

(ϕ_e O/F) = 10/11 = 0.909 *i.e.,* for every one mole of $Ca(NO_3)_2$, 0.909 mole acetamide required.

(ϕ_e O/F) = 10/11 = 0.909 *i.e.,* for every one mole of $Zn(NO_3)_2$, 0.909 mole acetamide required.

For the synthesis of $CaZnO_2$-II the total number of moles of acetamide required is: 0.909+0.909= 1.818 mole (Fig. 3).

Fig. 3. Synthesized CaZnO$_2$-II at 600 °C.

2.3. CHARACTERIZATION OF THE NANOPARTICLES

$CaZnO_2$ nanoparticles were characterized by XRD, SEM and UV absorption spectroscopy.

2.3.1. X-Ray Diffraction (XRD)

The powdered sample of $CaZnO_2$-I and $CaZnO_2$-II nanoparticles were examined by XRD and analysis was carried out on fresh sample to assess the purity of the expected phases and the degree of crystallization i.e., size, composition and crystal structure.

XRD was performed by Rigaku diffractometer using Cu-K$_\alpha$ radiation (1.5406 Å) in a θ-2θ configuration [25]. According to the Debye Scherrer's formula:

$$D = \left(K\lambda / \beta \cos\theta \right)$$ (1)

where: D = thickness of the crystallite
                  K = 0.90 the Scherrer's constant (dependent on crystallite shape)
                  λ = X-ray wavelength
                  β = the peak width at half-maximum (FWHM)
                  θ = the Bragg diffraction angle

In the present work, the powdered sample of newly synthesized $CaZnO_2$-I and $CaZnO_2$-II nanoparticles were examined by using XRD and the average crystallite size of $CaZnO_2$-I was found to be 39 nm and similarly $CaZnO_2$-II was found to be 44 nm.

2.3.1.1. X-Ray Diffraction studies of CaZnO$_2$-I and CaZnO$_2$-II

The powdered sample of $CaZnO_2$-I nanoparticle was examined by XRD and analysis was carried out on fresh sample to assess the purity of the expected phases and the degree of crystallization i.e., size, composition and crystal structure. XRD was performed by Rigaku diffractometer using Cu-K$_\alpha$ radiation (1.5406 Å) in θ -2θ configuration. According to the XRD the average crystallite size of $CaZnO_2$-I and $CaZnO_2$-II were found to be 39 nm (Fig. 4) and 44 nm (Fig. 5) respectively.
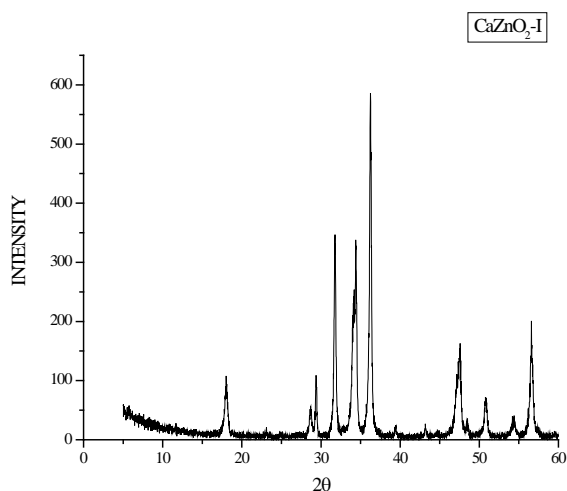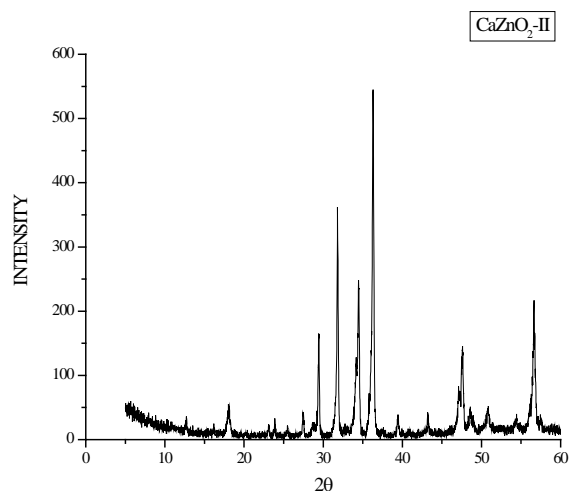
Fig. 4. X-Ray Diffraction of CaZnO₂-I.

Fig. 5. X-Ray Diffraction of CaZnO₂-II.

2.3.2. Scanning Electron Micrograph (SEM)

In the present work powdered sample of $CaZnO_2$-I and $CaZnO_2$-II nanoparticles were examined by using SEM technique. The study of the surface of the nanoparticle gives valuable information about its internal structure.

2.3.2.1. SEM study of CaZnO₂-I

The SEM images illustrate that, the mixture of both rod like structures and plates with amorphous powder which have been tightly packed in a groups. The enlarged image shows the different particle groups attached together (Fig. 6).

Fig. 6. SEM photograph of CaZnO₂-I.

2.3.2.2. SEM STUDY OF CaZnO₂-II

The SEM images show the common mixture of rod like structures and plates with crystals in a tightly packed in groups. The enlarged image shows the compact groups attached together (Fig.7).
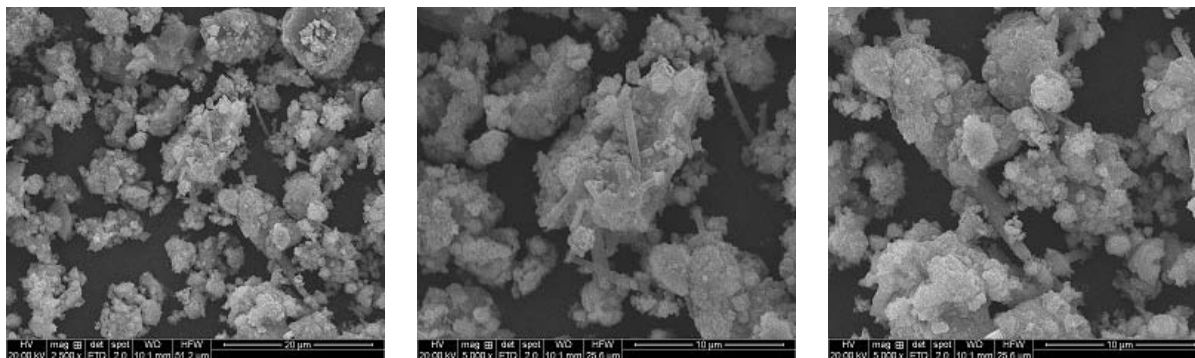
Fig. 7. SEM photograph of CaZnO₂-II.

2.3.3. UV ABSORPTION SPECTROSCOPY

Absorption spectra of the CaZnO$_2$-I and CaZnO$_2$-II metal oxide nanoparticles were recorded using UV-VIS spectrophotometer (Ocean Optics DH-2000) over the wavelength range 200-1200nm at Nano Research Laboratory, Department of Nanotechnology, Kuvempu University. From this spectrum, it has been inferred that the nanoparticles have sufficient transmission in the entire visible and IR region.

The band gap energy of the CaZnO$_2$-I and CaZnO$_2$-II nanoparticles was calculated using the following simple conversion equation. The band gap equation is calculated using the Planck's equation as follows.

$$E = hC / \lambda$$

where h = Planck's constant ($h = 4.135 \times 10^{-15} eV$),
C = velocity of light (speed of light) ($C = 3 \times 10^8 m/s$),
λ = wavelength of light ($\lambda = ... \times 10^{-9} m$)

$$\text{Band gap energy } (eV) = 4.135 \times 10^{-15} \times 3 \times 10^8 \times 10^9 / \lambda(m)$$
$$\text{Band gap energy } (eV) = 1240 / \text{wavelength } (m)$$

(2)

In the present work powdered sample of CaZnO$_2$-I and CaZnO$_2$-II metal oxide nanoparticles were examined by using UV absorption studies.

Fig. 8. UV absorption of CaZnO₂-I.
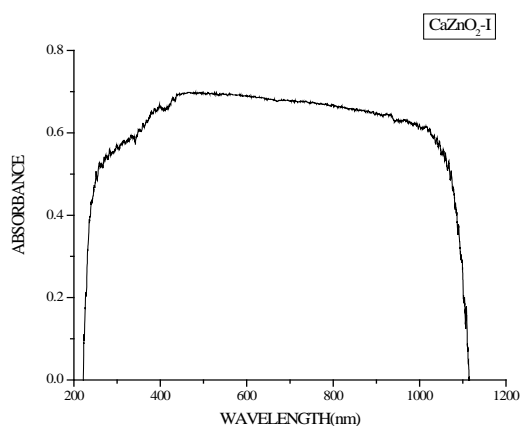

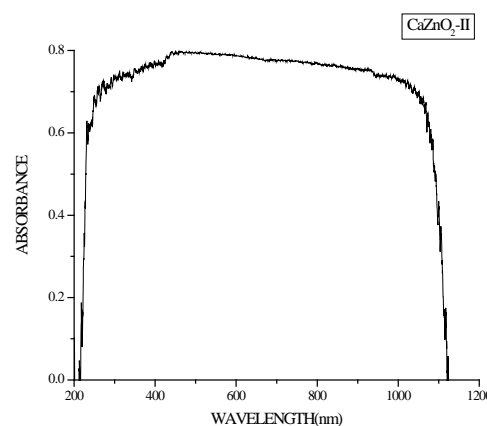**Fig. 9. UV absorption of CaZnO₂-II.**

Table 3. Band gap energy of CaZnO$_2$-I nanoparticles.

Band gap Energy (eV)	Nanoparticle	λ_{max} (nm)
2.5	CaZnO$_2$-I	481

Table 4. Band gap energy of CaZnO$_2$-II nanoparticles.

Nanoparticle	λ_{max} (nm)	Band gap Energy (eV)
CaZnO$_2$-II	464	2.6

The band gap energy of CaZnO$_2$-I is found to be 2.5 eV (Fig. 8) (Table 3) and CaZnO$_2$-II is found to be 2.6 (Fig. 9) (Table 4). With this we can say that the band gap of the semiconductors has been found to be particle size dependent [26].

3. RESULTS AND DISCUSSION

3.1. PHOTOCATALYTIC EXPERIMENTAL PROCEDURE: INITIAL STUDY OF THE TEXTILE EFFLUENT

Raw wastewater sample was collected from homogeneous tank of textile industry. Initially, sample was analyzed for some primary parameters like pH, Temperature, Odour, Colour, and COD. As the collected textile wastewater was highly concentrated, the sample was diluted with potable water before photocatalytic decolourization. The values of various wastewater parameters before treatment are shown in Table 5.

Table 5. Characteristics of raw wastewater from textile industry.

Sl. No.	Parameter	Value
1	pH	10.3
2	Temperature	36°C
3	Odour	Unpleasant
4	COD	2202 mg/L
5	Colour	Black

3.2. PHOTOCATALYTIC EXPERIMENTAL PROCEDURE: COMPARATIVE STUDY OF PHOTOCATALYTIC DECOLOURIZATION OF COLOURED TEXTILE EFFLUENT USING THE CaZnO$_2$-I AND CaZnO$_2$-II NANOPARTICLES OVER PROCURED TiO$_2$

Photocatalytic experiments were carried out in presence of direct sunlight of intensity between 100000 to 130000 lux (recorded by using TES 1332A digital Lux meter). The experiments were carried out between 10 am to 1 pm and 3 ml of raw effluent was diluted 1000ml of potable water to make the aqueous solution of 3% concentration. In all photocatalytic experiments, 100 ml of 3% textile effluent solution was taken in 100 ml Borosil beakers. The UV-VIS spectrophotometer 119 (Systronics) was used for the determination of absorbance in the range of 200 to 800nm. The λ_{max} of textile effluent was found to be 440 nm. A known amount of dosage (0.5g/100ml) of the different nanoparticles; TiO$_2$, CaZnO$_2$-I and CaZnO$_2$-II were added to six different beakers containing textile effluent solution and the beakers were kept in the sunlight for photocatalytic activity. Further

experiments were conducted based on the decolourization results obtained from the photocatalytic activity of the catalysts.

3.3. EFFECT OF PHOTOCATALYSTS ON PHOTOCATALYTIC DECOLOURIZATION OF TEXTILE EFFLUENT

Blank experiments were performed under direct sunlight without the addition of catalysts and no decolourization was observed. A known concentration of TiO_2, $CaZnO_2$-I and $CaZnO_2$-II (0.5g/100ml) were added to six beakers containing textile effluent solution and kept in the sunlight for photocatalytic activity. The results showed that the nanoparticles ($CaZnO_2$-I and $CaZnO_2$-II) have exhibited higher photocatalytic activity than TiO_2. A decolourization of 15.60% was recorded for TiO_2 nanoparticle and 95.54% for $CaZnO_2$-I and 94.85% for $CaZnO_2$-II were recorded (Fig. 10) (Photo 1).
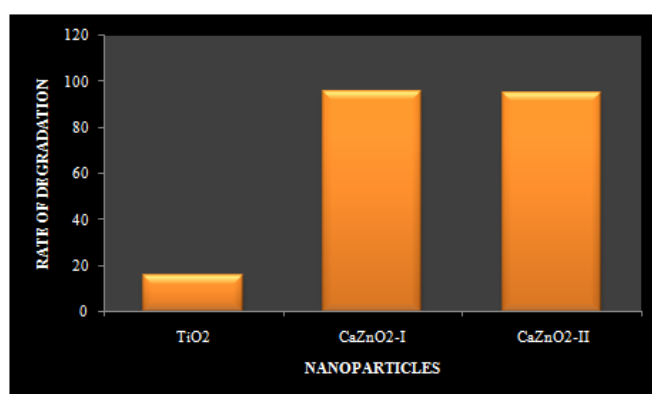

Fig. 10. Rate of degradation of textile effluent at 120 minutes [textile effluent =3%, pH=7, TiO_2=0.5g, $CaZnO_2$-I=0.5g, $CaZnO_2$-II=0.5g].

<div align="center">(a)   (b)</div>

Photo 1. Rate of degradation of textile effluent at 120 minutes [(a)=Tex.eff./TiO_2/ $CaZnO_2$-I, (b)=Tex.eff./TiO_2/$CaZnO_2$-II].

Both the synthesized nanoparticles have exhibited higher photocatalytic activity than the commercially available TiO_2. Photocatalytic decolourization of the azo dye is mainly due to the hydroxyl radical attack on the dye molecule [27]. The production of hydroxyl radicals of the TiO_2 catalyst may be very less when compared with the synthesized nanoparticles which have exhibited high degradation in presence of sunlight. Based on the results further studies were done concentrating on the synthesized $CaZnO_2$-I and $CaZnO_2$-II nanoparticles.

3.4. PHOTOCATALYTIC EXPERIMENTAL PROCEDURE: STUDY ON PHOTOCATALYTIC DECOLOURIZATION OF TEXTILE EFFLUENT USING CaZnO$_2$-I AND CaZnO$_2$-II NANOPARTICLES

In the second stage, the synthesized nanoparticles were continued for the photocatalytic degradation studies. Photocatalytic suspensions from 0.1 g, 0.2 g, 0.3 g up to 1g were tested on the 100 ml textile effluent samples. The suspension pH values were adjusted by using NaOH/HCl solutions using pH meter. Before irradiation, photocatalyst suspension was stirred in the dark to ensure the adsorption equilibrium and was kept in sunlight for the photocatalytic decolourization. At an interval of 30 minutes the suspension was sampled and centrifuged (EBA-Hetlich) at 3000 rpm for 5 minutes to remove photocatalyst particles. The residual concentration of the solution samples was monitored by using UV-VIS spectrophotometer 119 (Systronics) at 440 nm. The experiments were conducted for different pH range from 2 to 11 in order to study the efficiency of the nanoparticles in Acidic, Alkaline and Neutral conditions. The data obtained from the photocatalytic degradation experiments were used to calculate the degradation efficiency 'D' (Eq. 3).

$$D = \left(A_0 - A_t / A_0 \right) \times 100 \tag{3}$$

where A_0 is the initial absorbance of dye solution
            A_t is absorbance at time 't'.

3.5. EFFECT OF CATALYST CONCENTRATION ON TEXTILE EFFLUENT

The effect of catalyst concentration on photocatalytic degradation was studied over a range of catalyst amount from 0.1 to 1g/100ml for the textile effluent. Both the synthesized nanoparticles have shown appreciable results. Where, CaZnO$_2$-I showed 96.39% for the 0.6g/100ml and CaZnO$_2$-II showed 94.85% at 0.7g/100ml in 120 minutes (Fig. 11) (Photo 2).
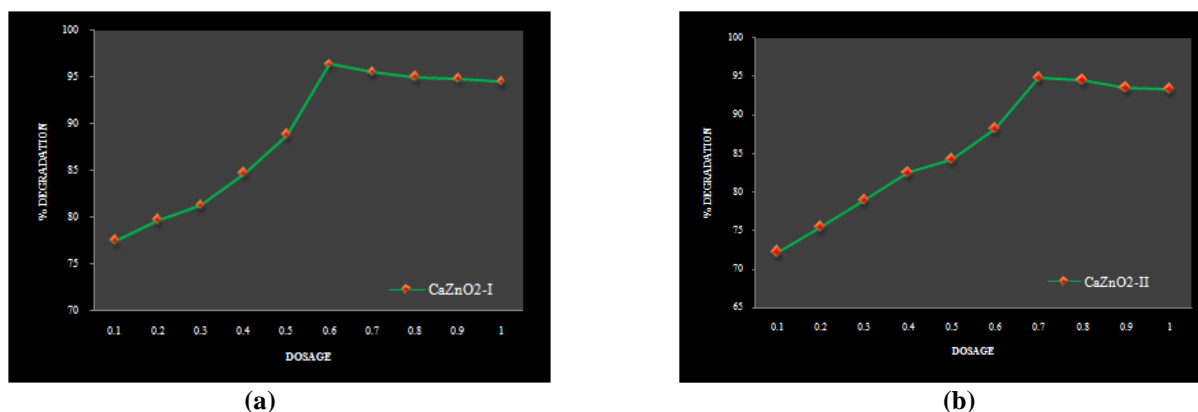

| (a) | (b) |

Fig. 11. Effect of catalyst concentration on textile effluent at 120 minutes [textile effluent=3% at pH=7, (a)=CaZnO$_2$-I, (b)=CaZnO$_2$-II].

(a)   **(b)**

Photo 2. Effect of catalyst concentration on textile effluent at 120 minutes [textile effluent=3% at pH=7, (a)=CaZnO$_2$-I, (b)=CaZnO$_2$-II].

The increase in decolourization rate can be explained in terms of availability of active sites on the catalyst surface and sunlight penetration into the suspension as a result of increased screening effect and scattering of light. Further increase in the catalyst amount beyond the optimum dosage for all the nanoparticles decreases the decolourization by some margin. This may be due to overlapping of adsorption sites as a result of overcrowding owing to collision with ground state catalyst [28]. Since the decolourization was most effective at 0.6 g/ 100 ml for CaZnO$_2$-I and 0.7 g/100 ml for CaZnO$_2$-II nanoparticle dosages, the following experiments were continued with same dosages.

3.6. MECHANISM OF THE PHOTOCATALYTIC DECOLOURIZATION

The mechanism of photocatalytic activity of the used catalyst nanoparticle is predicted as follows. Under sunlight irradiation catalyst molecules get excited and transfer electron to the conduction band (Eq. 4).

$$\text{Nanoparticles} + h\nu \rightarrow (e^-_{CB} + h^+_{VB}) \tag{4}$$
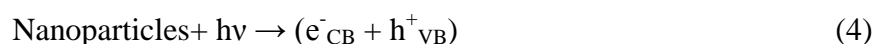
Electron in the conduction band of the catalyst can reduce molecular oxygen and produce the super oxide radical (Eq. 5).

$$e^-_{CB} + O_2 \rightarrow O_2^{\bullet-} \tag{5}$$

Molecular oxygen, adsorbed on the surface of the photocatalyst prevents the hole-electron pair recombination process [29-30]. Recombination of hole-electron pair decreases the rate of photocatalytic degradation. This radical may form hydrogen peroxide or organic peroxide in the presence of oxygen and organic molecule (Eqs. 6, 7, 8).

$$H_2O + O_2^{\bullet-} \rightarrow OOH^\bullet + OH^- \tag{6}$$
$$2OOH^\bullet \rightarrow O_2 + H_2O_2 \tag{7}$$
$$O_2^{\bullet-} + \text{textile effluent} \rightarrow \text{textile effluent -OO}^\bullet \tag{8}$$

Hydrogen peroxide can be generated in another path (Eq. 9).

$$OOH^\bullet + H_2O + e^-_{CB} \rightarrow H_2O_2 + OH^- \tag{9}$$

Hydrogen peroxide can form hydroxyl radicals which are powerful oxidizing agents (Eqs. 10, 11).

$$H_2O_2 + e^-_{CB} \rightarrow OH^\bullet + OH^- \tag{10}$$
$$H_2O_2 + O_2^{\bullet-} \rightarrow OH^\bullet + OH^- + O_2 \tag{11}$$
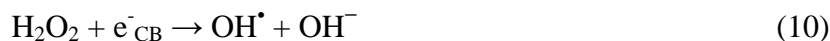
The radicals produced are capable of attacking textile effluent molecules and decolourize them (Eq. 12).

$$OH^\bullet/O_2^{\bullet-}/Nanoparticles^{\bullet+} + \text{textile effluent} \rightarrow \text{textile effluent decolourization} \tag{12}$$
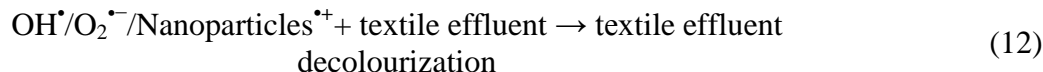
3.7. EFFECT OF pH ON TEXTILE EFFLUENT

In order to study the effect of pH on the decolourization efficiency of $CaZnO_2$-I and $CaZnO_2$-II catalysts, the experiments were conducted at pH ranging from 2 to11. The results showed that, pH significantly affected the decolourization efficiency (Fig. 12) (Photo 3).
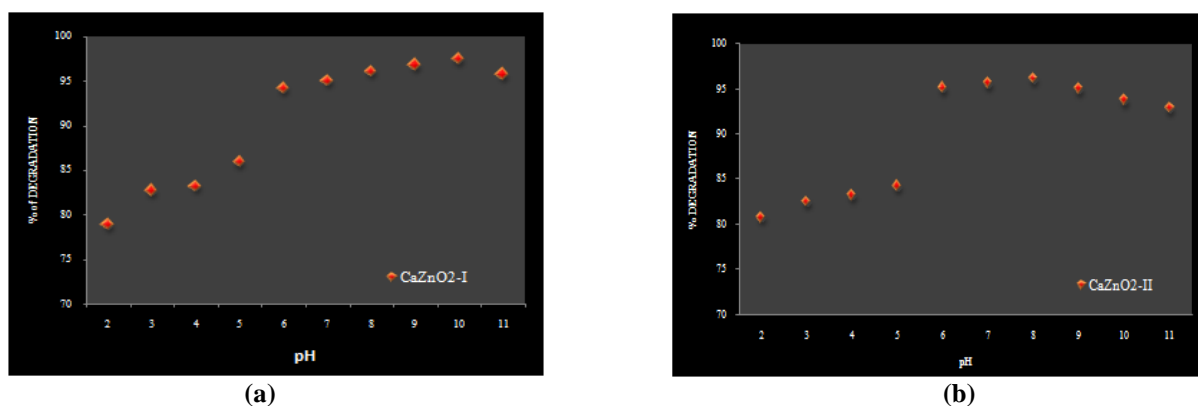

(a)   (b)

Fig. 12. Effect of pH on the photocatalytic degradation of textile effluent at 120 minutes [textile effluent =3%, (a)= CaZnO₂-I, (b)=CaZnO₂-II].

(a)

(b)

Photo 3. Effect of pH on the photocatalytic degradation of textile effluent at 120 minutes [textile effluent =3%, (a)= CaZnO₂-I, (b)=CaZnO₂-II].

The decolourization rate of textile effluent for $CaZnO_2$-I, the decolourization increased from 78.90% to 97.42% from pH 2 to 10 and decreased to 95.71% at 11 in 120 minutes for 0.6 g/100 ml and for $CaZnO_2$-II the decolourization of the effluent increased from 81% to 96% form pH 2 to pH 8 and decreased to 93% at pH 11 for 0.7 g/100 ml. The maximum decolourization rate for all different nanoparticles was achieved at pH 10, 8. As the collected effluent maybe having the anionic dyes which results in more efficient formation of hydroxyl radicals in alkaline medium. Excess of hydroxyl anions increases the formation of $OH^\bullet$ radicals. These $OH^\bullet$ radicals are the main oxidizing species responsible for photocatalytic

decolourization [31]. Above optimum pH, the decrease in decolourization efficiency can be explained on the basis of amphoteric nature of the catalysts. The catalyst surface becomes negatively charged for higher pH values, which causes the electrostatic repulsion between the catalyst and negatively charged dyes [32].

3.8. EFFECT ON DIFFERENT CONCENTRATION OF TEXTILE EFFLUENT

The initial concentration of textile effluent was varied from 3%, 6%, 9% and 12% to study the effect on different concentrations of textile effluent. The decolourization results obtained for $CaZnO_2$-I obtained 97.42%, 95.49%, 54.42% and 29.81% for the aqueous solution 3%, 6%, 9% and 12%. In the same way $CaZnO_2$-II resulted 96.05%, 70.34%, 33.91% and 7.15% for the following 3%, 6%, 9% and 12% textile effluent concentrations (Fig. 13) (Photo 4).
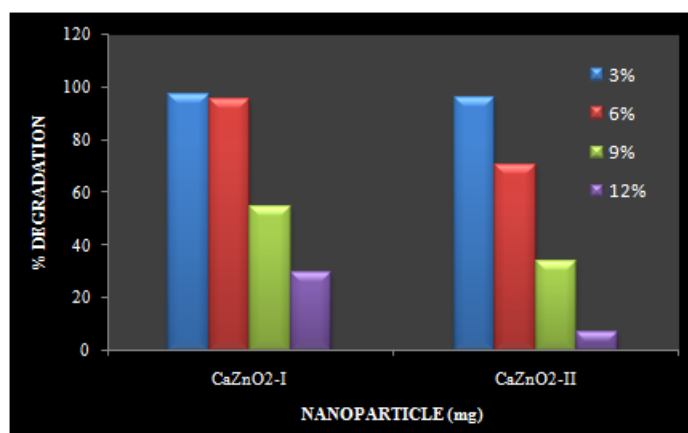

Fig. 13. Effect of initial dye concentration on photocatalytic degradation of textile effluent [$CaZnO_2$-I/pH= 0.6g/10, $CaZnO_2$-II/pH=0.7g/8].

(a)

(b)

Photo 4. Effect of initial dye concentration on photocatalytic degradation of textile effluent [(a)=$CaZnO_2$-I/pH= 0.6g/10, (b)=$CaZnO_2$-II/pH= 0.7g/8].

These series of experiments illustrated that the decolourization efficiency was inversely affected by the concentration. The decrease in the decolourization with increase in effluent concentration was ascribed to the equilibrium adsorption of dye on the catalyst surface which results in decrease in the active sites This phenomenon results in the lower formation of $OH^{\bullet}$ radicals which were considered as primary oxidizing agents of the organic dye [33]. According to Beer Lambert law, as the initial dye concentration increases, the path length of photons entering the solution decreases. This results in lower photon adsorption on the catalyst particles, and consequently decreases photocatalytic reaction rate [34].

3.9. EFFECT OF SUNLIGHT IRRADIATION ON TEXTILE EFFLUENT

Sunlight irradiation generates the photons required for the electron transfer from the valence band to the conduction band of a semiconductor photocatalyst. The energy of a photon is related to its wavelength and the overall energy input to a photocatalytic process is dependent on the light intensity. Therefore, the effects of both intensity and wavelength are important. In the present study, the effect of the sunlight intensity was studied by keeping the constant wavelength (440nm).

The photocatalytic decolourization of diluted textile effluent (*i.e.*, 3%) conducted under three different experimental conditions were examined, *i.e.*, under sunlight alone, textile effluent/dark/catalyst and textile effluent/sunlight/catalyst for all the different catalysts. When textile effluent solution was exposed directly to the sunlight, the decolourization was found to be nil during the entire experiments. The decolourization rate was found to increase with increase in irradiation time, for textile effluent/sunlight/$CaZnO_2$-I recorded 97.42% and textile effluent/dark/$CaZnO_2$-I 27.78% was recorded. The textile effluent/sunlight/$CaZnO_2$-II achieved 96.05% and textile effluent/dark/$CaZnO_2$-II 21.61% was recorded with 120 minutes respectively (Fig. 14) (Photo 5).
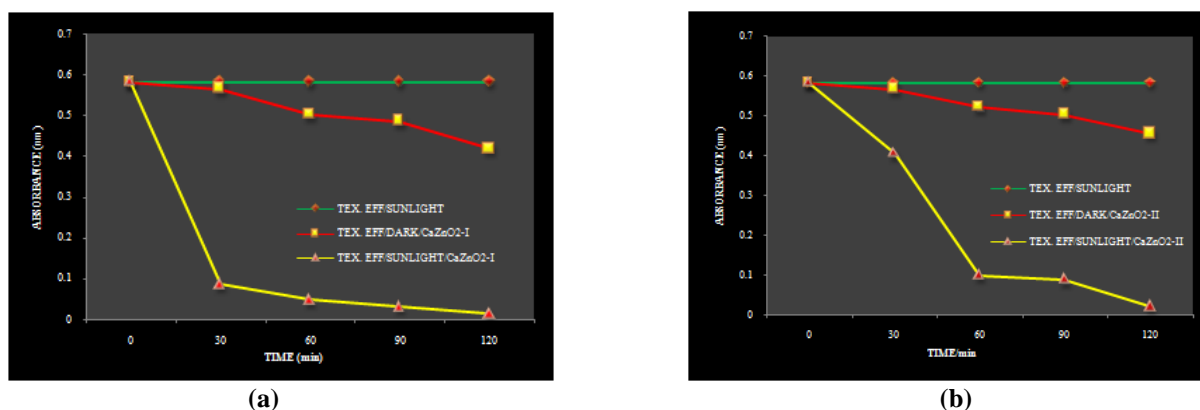

(a)   **(b)**

Fig. 14. Effect of sunlight irradiation on photocatalytic degradation of textile effluent in 120 minutes. [(a) =$CaZnO_2$-I at pH 10, (b) =$CaZnO_2$-II at pH 8].

(a)   **(a1)**

(b)   **(b1)**

Photo 5. Effect of sunlight irradiation on photocatalytic degradation of textile effluent in 120 minutes.
[(a)=tex.eff./sunlight/$CaZnO_2$-I at pH 10, (b)=tex.eff./sunlight/$CaZnO_2$-II at pH 8]
[(a1) =tex.eff./dark/$CaZnO_2$-I at pH 10, (b1) =tex.eff./dark/$CaZnO_2$-II at pH 8].

These results clearly showed that, decolourization occurs more efficiently in presence of sunlight. Under sunlight excitation of catalysts takes place rapidly than in absence of light. The experiment demonstrated that, both sunlight and photocatalyst are needed for the effective destruction of textile effluent, as it has been established that the photocatalytic decolourization of organic matter in the effluent is initiated by the photo excitation of the semiconductor, followed by the formation of electron hole pair on the surface of the catalyst.

4. CONCLUSIONS

Release of coloured textile effluents is undesirable in the aquatic environment as it limits the utilization of the water resources. Photocatalytic decolorization is an alternative method to other conventional inefficient physico-chemical and biological methods to treat toxic effluents. The feasibility of photocatalytic decolourization and degradation of the effluent, was studied by using the synthesized metal oxide nanoparticles as photocatalysts.

The synthesized photocatalysts have shown a maximum decolourization of the selected effluent under solar radiation. Among the catalysts used except TiO_2 all the other nanoparticles $CaZnO_2$-I and $CaZnO_2$-II were proved to be very efficient photocatalysts in decolorizing the azo dye and achieving 95.54% and 94.85% respectively in 120 minutes at pH 7. The synthesized nanoparticles have been more efficient than the procured nanoparticle TiO_2 which could able to achieve only 15.60% of decolourization in 120 minutes at pH 7.

Similarly, when the pH was altered, 97.42% at pH 10 for 0.6g/100ml and 96% at pH 8 for 0.7g/100ml to the following $CaZnO_2$-I and $CaZnO_2$-II metal oxide nanoparticles. Hence, the obtained results have proved that, photocatalytic decolourization of textile effluent was mainly dependent on the pH of the dye solution and catalyst dosage. The textile effluent achieved high colour removal in alkaline medium. The results also revealed that, the sunlight is most efficient source for the photocatalytic activity.

REFERENCES

[1]   Bell, J., Buckley, C.A., *Water SA,* **29**(2), 129, 2003.
[2]   McMullan, G., Meehan, C., Conneely, A., Kirby, N., Robinson, T., Nigam, P., Banat, I.M., Marchant, R., Smyth, W.F., *Applied Microbiology and Biotechnology,* **56**, 81, 2001.
[3]   Arslan, I., Balcioglu, I.A., Bahnemann, D.W., *Applied Catalysis B,* **26**, 193, 2000.
[4]   Sauer, T., Neto, G.C., Jose, H.J., Moreira, R.F.P.M., *Journal of Photochemistry and Photobiology A: Chemistry,* **149**, 147, 2002.
[5]   Sreedhar, R.S., Kotaiah, B., Siva Prasad Reddy, N., Velu, M., *Turkish Journal of Engineering and Environmental Science,* **30**, 367, 2006.
[6]   Saggioro, E.M., Oliveira, A.S., Pavesi, T., Maia, C.G., Ferreira, L.F.V., Moreira, J.C., *Molecules,* **16**, 10370, 2011.
[7]   Malato, S., Blanco, J., Vidal, A. Richter, C., *Applied Catalysis B: Environmental,* **37**, 1, 2002.
[8]   Yeber, M.C., Rodriguez, J., Freer, J., Duran, N., Mansilla, H.D., *Chemosphere,* **41**, 1193, 2000.
[9]   Behnajady, A., Modirshahla, N., Hamzavi, R., *Journal of Hazardous Materials B,* **133**, 226, 2006.

[10]   Khodja, A.A., Sehili, T., Pilichowski, J.F., Boule, P., *Journal of Photochemistry and Photobiology A: Chemistry,* **141**, 231, 2001.

[11]   Lizama, C., Freer, J., Baeza, J., Mansilla, H.D., *Catalysis Today,* **76**, 235, 2002.

[12]   Gouvea, C.A.K., Wypych, F., Moraes, S.G., Duran, N., Nagata, N., Peralta-Zamora, P., *Chemosphere,* **40**, 433, 2000.

[13]   Madhusudhana, N., Yogendra, K., Mahadevan, K.M., *International Journal of Engineering Research and Applications,* **2**, 1300, 2012.

[14]   Madhusudhana, N., Yogendra, K., Mahadevan, K.M., *Research Journal of Chemical Sciences,* **2**, 72, 2012.

[15]   Madhusudhana, N., Yogendra, K., Mahadevan, K.M., Suneel Naik, *International Journal of Chemical Engineering Applications,* **2**, 301, 2011.

[16]   Madhusudhana, N., Yogendra, K., Mahadevan, K.M., Suneel Naik, Gopalappa, H., *Environmental Science: An Indian Journal,* **6**, 1, 2011.

[17]   Yogendra, K., Suneel Naik, Mahadevan, K.M., Madhusudhana, N., *International Journal of Environmental Science and Research,* **1**, 11, 2011.

[18]   Yogendra, K., Mahadevan, K.M., Suneel Naik, Madhusudhana, N., *International Journal of Environmental Sciences,* **1**, 839, 2011.

[19]   Gopalappa, H., Yogendra, K., Mahadevan, K.M., Madhusudhana, N., *International Journal of Science Research,* **1**, 91, 2012.

[20]   Gopalappa, H., Yogendra, K., Mahadevan, K.M., Madhusudhana, N., *International Journal of Universal Pharmacy and Life Sciences,* **2**, 66, 2012.

[21]   Mimani, T., Patil, K.C., *Materials Physics and Mechanics,* **4**, 134, 2001.

[22]   Deshpande, K., Mukasyan, A.M., Varma, A., *Chemistry of Materials,* **16**, 4896, 2004.

[23]   Kingsley, J.J., Manickam, N., Patil, K.C., *Bulletin of Material Sciences,* **13**, 179, 1990.

[24]   Kingsley, J.J., Suresh, K., Patil, K.C., *Journal of Materials Science,* **25**, 1305, 1990.

[25]   Girase, K.D., Patil, H.M., Sawant, D.K., Bhavsar, D.S., *Archives of Applied Science Research,* **3**, 128, 2011.

[26]   Sawant, D.K., Patil, H.M., Bhavsar, D.S., Patil, J.H., Girase, K.D., *Archives of Physics Research,* **2**, 67, 2011.

[27]   Giwa, A., Nkeonye, P.O., Bello, K.A., Kolawole, E.G., Oliveira Campos, A.M.F., *International Journal Applied Science and Technology,* **2**, 90, 2012.

[28]   Subramani, A.K., Byrappa, K., Ananda, S., Lokanatha Rai, K.M., Ranganathaiah, C., Yoshimura, M., *Bulletin of Material Sciences,* **30**, 37, 2007.

[29]   Di-Paola, A., Augugliaro, V., Palmisano, L., Pantaleo, G., Savinov, E., *Journal of Photochemistry and Photobiology A: Chemistry,* **155**, 207, 2003.

[30]   Da-Silva, C.G., Faria, J.L., *Journal of Photochemistry and Photobiology A: Chemistry,* **155**, 133, 2003.

[31]   Noorjahan, M., Pratap Reddy, M., Durga Kumari, V., Lavedrine, B., Boule, P. Subrahmanyam, M., *Journal of Photochemistry and Photobiology A: Chemistry,* **156**, 179, 2003.

[32]   Turchi, C.S., Ollis, D.F., *Journal of Catalysis,* **122**, 178, 1990.

[33]   Mirkhani, V., Tangestaninejad, S., Moghadam, M., Habibi, M.H., Rostami Vartooni, A., *Journal Iranian Chemical Society,* **6**, 578, 2009.

[34]   Byrappa, K., Subramani, A.K., Ananda, S., Lokanatha Rai, K.M., Dinesh, R., Yoshimura, M., *Bulletin of Material Sciences,* **29**, 433, 2006.